Velocity Measurements In The Vapour Channel Of Low_Temperature Range Heat Pipes

A. V. Seryakov

Scientific laboratory, Special Relay System Design and Engineering Bureau,
Nekhinskaya Street, 55, 173021, Velikiy Novgorod, Russia.

This work presents part calculation and part experimental research of heat-transfer characteristics intensification of medium-temperature heat pipes. A vapour jet nozzle is used, similar to the Laval nozzle, surrounded by a capillary-porous insert along the full length of the heat pipe. This is axial to the direction of heat flow, and increases the velocity of the vapour flow.

Key words: Low-temperature range heat pipes, capillary-porous insert, capillary vapour injectors, Laval nozzle.

The intensification of heat-transfer characteristics of medium temperature range heat pipes (HP), which are used to cool heat-loaded elements in electronics, including spacecraft electronics, is a current problem. Heat-transfer efficiency and operational effectiveness of HPs with capillary-porous inserts are defined by the closed circulation motion of the heat conductor, which undergoes liquid-vapour transition and heat absorption in the evaporation region of the capillary porous insert, vapour phase transfer though convergent-divergent vapour channel, vapour-liquid transition with the liberation of heat in the condensation region, and liquid return to the evaporation region through the capillary-porous inserts of the HP.

To estimate maximum values of heat transport capabilities and working fluid selection, the fluid quality parameter is used, which is defined according to the expression:

$$\psi = \frac{\rho \cdot r \cdot \sigma}{\mu} \qquad (1)$$

where: ψ is the quality parameter of working fluid, W/sm^2 **(**10^4 W/m^2**)**; ρ- density, kg/m^3; r- latent evaporation heat , kJ/kg; σ- surface tension coefficient, N·m; μ - dynamic viscosity coefficient, Pa·s; of working fluid.

Fig.1 shows temperature dependencies of the quality parameter ψ of working fluid range usable for medium temperature heat pipes.

Calculations of the ψ parameter were carried out according to available thermophysical data with the use of degree interpolation. It is obvious that the temperature range of working fluid use is narrow and generally doesn't exceed 300°C.

The diethyl ether $C_4H_{10}O$ is selected as a main working fluid, which has boiling temperature at atmospheric pressure of T_B =35.4°C, freezing temperature T_F = −116.2°C and critical parameters T_C =193.4°C, P_C =3.61MPa.

Successful use of diethyl ether as a working fluid for Wilson chambers [7], with a long-duration liquid phase at 140°C, shows its heat resilience, and allows using it as a HP working fluid.

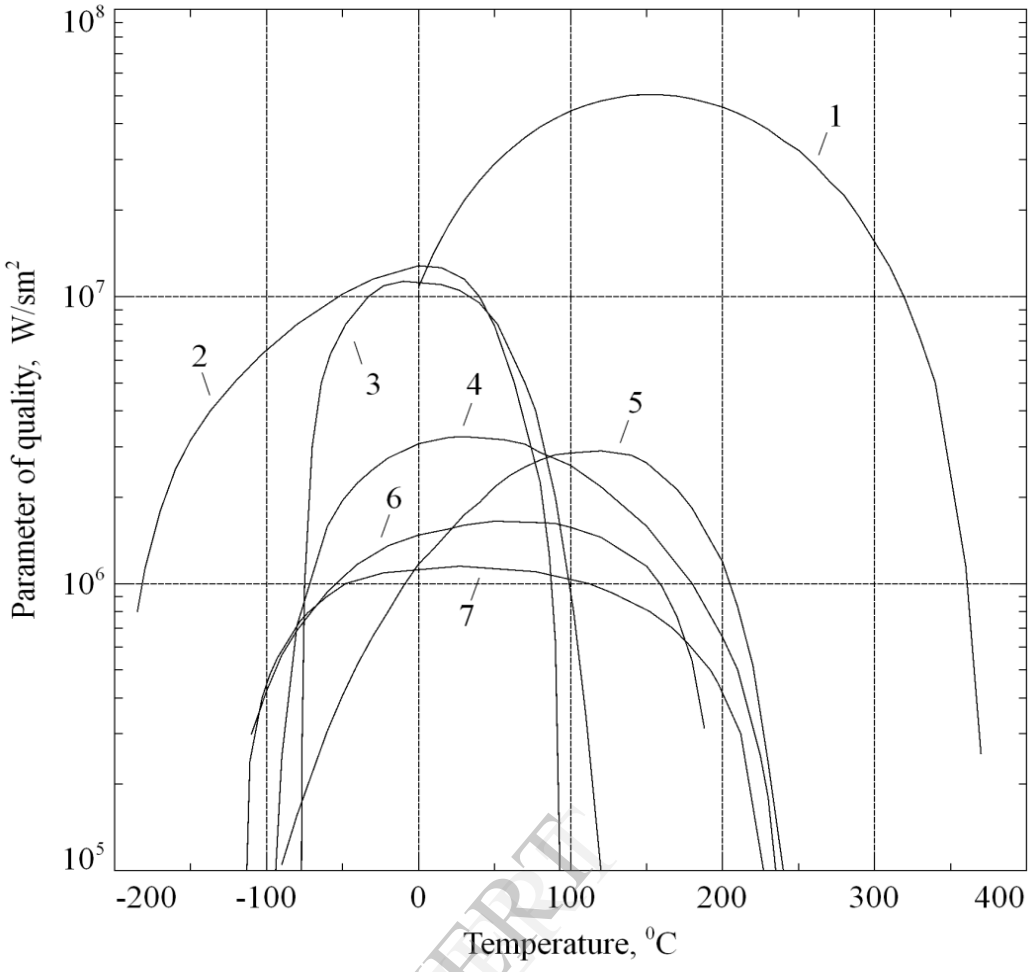

Fig.1. Quality parameter ψ, W/sm^2 , of working fluids: 1 – water H_2O; 2 – propylene C_3H_6; 3 – ammonia NH_3; 4 – acetone C_3H_6O; 5 – ethanol C_2H_5OH; 6 – diethyl ether $C_4H_{10}O$; 7 – methanol CH_3OH.

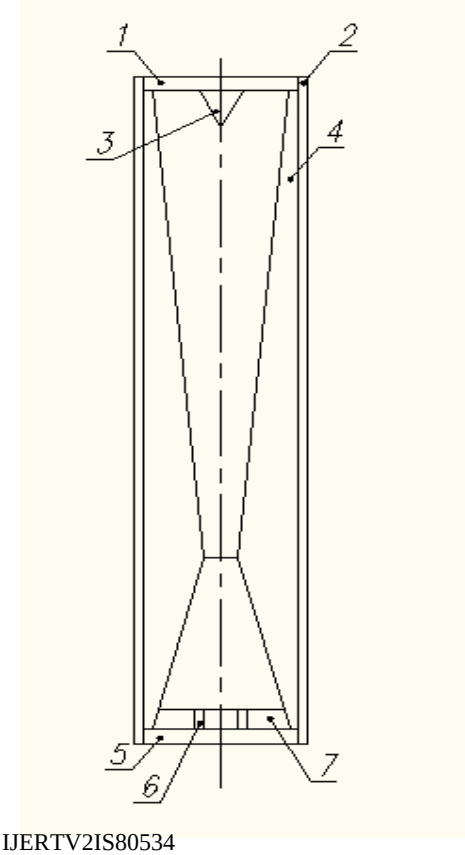

In the axial direction of heat flow, typical for short HP, the preferable design solution is a metal capillary-porous flat evaporator welded on the flat bottom cover and equipped with injector vapour channels.

Fig.2 shows a HP circuit with flat evaporator, convergent-divergent vapour channel and turbulator [8-12]. Length of HP is 100 mm, the diameter is 20 mm.

Fig. 2. Heat pipe diagram

1 – top cover; 2 – cylinder body of the HP; 3 – cone-shaped turbulator; 4 – capillary-porous insert; 5 – bottom cover; 6 – capillary injector channels, 7 – bottom flat capillary-porous insert-evaporator.

In stainless steel HPs with small diameter it is possible to use flat covers due to their moderate thermal resistance and easy fabrication.

The vapour phase transfer goes through the vapour channel arranged along the central axis of the capillary-porous insert, which in its turn is firmly mounted and mechanically fixed in a thin-wall cylindrical body with top and bottom covers.

The centrally arranged vapour channel, which is made in the form of a dynamic convergent-divergent nozzle, similar to the Laval nozzle, is

surrounded by a capillary-porous insert along the full length of the HP, which allows a significant reduction of heat losses.

Without the capillary-porous layer, noticeable cooling of the nozzle occurs due to external heat exchange processes, which leads to supersaturation of the vapour in a boundary layer alongside the nozzle closure. This results in a failure of the normal mode of the vapor jet outflow: premature appearance of a large number of microdrops of the working fluid condensate in the flow in the diffuser section near the throat. Thereby divergence of the vapor jet increases significantly, and it impinges on the walls of the capillary-porous insert, which reduces the maximum values of HP heat transfer parameters.

Condensation shocks, which occur in the divergent section of the nozzle, come with heat release and under the influence of two factors (thermal and geometric) the vapour flow can lose its stability.

The variable section of the capillary-porous insert, having maximum thickness near the nozzle throat section tapering toward the evaporation and condensation regions, protects the vapor flow from overcooling. Therefore condensation begins to occur only near the turbulator stagnation point and further on the inner surface of HP top cover at the stagnation temperature of the vapour flow, which exceeds evaporation temperature.

The overheating ΔT of the vapour flow at the nozzle exit, caused by the rise of stagnation temperature of the working fluid in the HP evaporator over its boiling temperature, is rated using the effective value of condensation heat by the formula [1-2]:

$$h_{eff} = h + C_p^{//} \cdot \Delta T \qquad (2)$$

where: h_{eff} – the effective value of condensation heat, kJ/kg; $C_P^{//}$ – vapor heat capacity, kJ/(kg·K); ΔT – difference between overheated vapour temperature and its saturation temperature at given pressure, K.

The overheating temperature ΔT under high thermal loads on the heat pipe reaches 0.5 – 1K.

The compression efficiency of the gas-dynamic convergent-divergent nozzle is the same as for Laval nozzle.

To intensify vaporization in the evaporation region under low thermal loads it is sensible to use some injector vapour discharge channels, through the capillary-porous insert-evaporator that is on the flat bottom cover of HP. The diameter of the injector channel is 1 mm, and reduced capillary pressure leads to a reduction of the boiling and vaporization temperatures of the working fluid in these channels. This is found to be a significant issue for HP functioning under low thermal loads and hence at low initial velocities of vapour flow over the evaporator.

The vapour flow velocity calculation was carried out using ANSYS. Navier-Stokes and heat-transfer equations with measured boundary conditions were solved, i.e. using fixed temperature values of heat source and heat outlet. The model was studied as a longitudinal section along the axes of the two injector channels, which helps to preserve all the specific features of whirling instability under the conditions of continuous circulation motion of the working fluid during liquid and vapor phases.

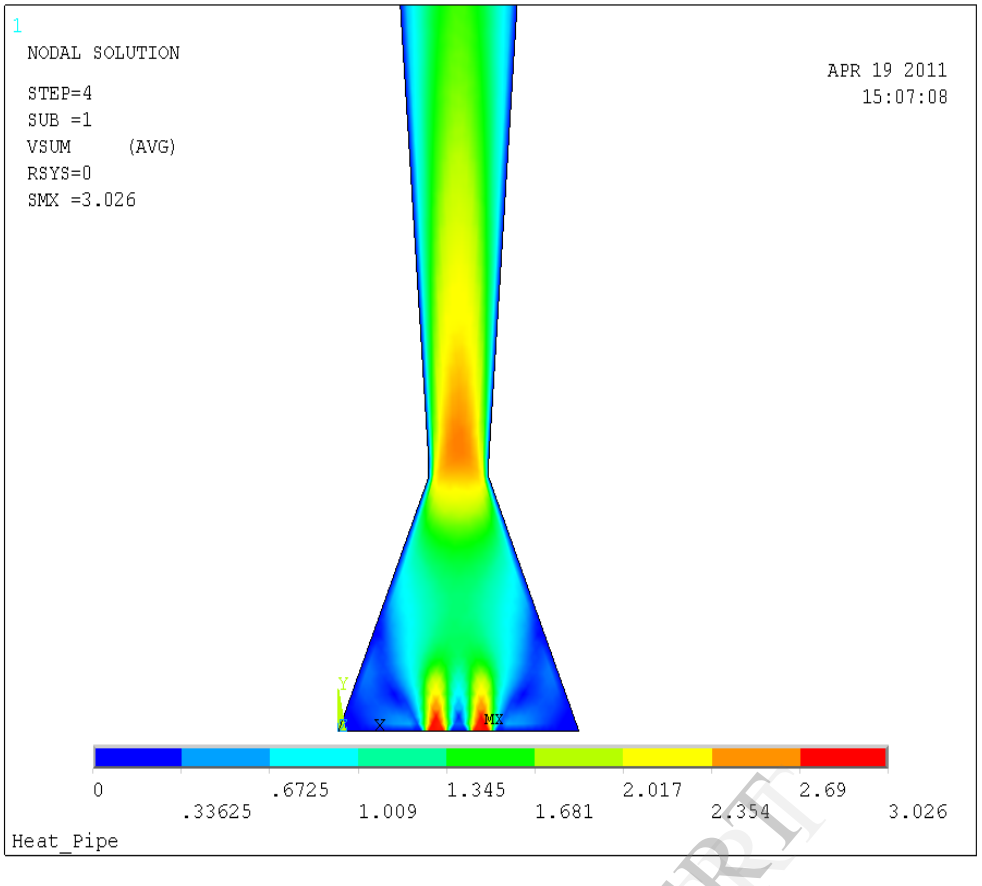

Fig. 3 shows the calculated vapour velocity distribution within HP, sm/s, over the injector vapour channels and in the Laval nozzle throat.

Fig.4 shows a more precise distribution value for the longitudinal component of velocity within the vapour channel HP calculated by the more capable program "CFD Design 10.0". One can see the accelerating influence and a sharp maximum of the velocity in the nozzle throat, with the velocity reducing in the diffuser part of HP and a smaller velocity increase near the turbulator frontal point.

Fig.4. Calculation results of longitudinal component of velocity of diethyl ether vapour along longitudinal axis of HP.

Experimental determination of the velocities of diethyl ether $C_4H_{10}O$ vapour flow were carried out at the nozzle throat with the help of a hot-wire anemometer [5,6]. A stainless steel tube-holder 6 mm in diameter and 15 mm in length, is welded on the outer surface of the HP body using laser-beam welding, perpendicular to the HP longitudinal axis, at the level of the nozzle throat. A screwed shank and external coupling nut with a tapering channel form the fixing mechanism for the hot-wire anemometer indicator.

The hot-wire anemometer indicator itself is a piece of a thin-walled kovar capillary tube of 2mm diameter and 0.05 mm thick walls, with current feedthroughs 0.3 mm in diameter covered with glass film. Sealing of the internal space of the capillary tube and anchoring of the current feedthroughs are achieved using glass powder C-48-5, inserted into the space inside the tube from one end using a continuous vibroflotation process, and which is sintered at 1000 ± 20°C temperature in a special mandrel. At one end of the tube at a depth of 5 – 6 mm an internal glass drop is formed, thus the current feedthroughs are reliably sealed, and at the opposite end of the tube a Teflon clamp with two openings for current feedthroughs is fixed. Then a small length of wire, as a sensing element, is welded on the current feedthroughs protruding from the glass drop using miniature welding machine CMC-6. The tungsten wire is 10 μm in diameter, resistance is $5.5 \cdot 10^{-8}$ Ω·m, temperature coefficient of resistance is $4.1 \cdot 10^{-3}$ 1/K.

The outer surface of the thin-walled capillary tube of the hot-wire anemometer is covered with a thin layer of a silicone sealant and inserted into the inner channel of the tube holder, and introduced into the vapour channel of the HP with a preset depth, so that the sensing wire is placed in the middle of the nozzle critical section, with orientation perpendicular to the longitudinal axis of the HP.

After sealer vulcanization and tightening of the union nut on the tube holder stem the HP is ready for degassing of the capillary porous insert, filling with working fluid and final sealing.

Calibration of the hot-wire anemometer was performed by experiment using a thermal siphon pipe hypsometer [7].

Pressure difference on the orifice meter was measured by means of a pressure-difference transducer Sapphire-22DD and micromanometer MMN-240. Diethyl ether was used as a working fluid of the siphon. During all measurements, the membrane block of the transducer Sapphire–22DD and feed lines were kept at 35°C temperature.

The hot-wire anemometer operating principle, within the working HP, is based on convective heat loss from the heated wire of the indicator in the saturated vapour flow. Electric heat P_0 generated by the wire, when heater current I_0 flows through anemometer is removed by convection P_{CONV} , conduction P_{COND} and radiative emission $P_{EM.}$ P_{EM} is neglected because of its low value at the given temperatures.

$$P_0 = P_{CONV} + P_{COND} \tag{3}$$

Conducted participation in the heat losses on the current input - termed called frame beams - of the hot-wire anemometer is estimated by the formula [1-4]

$$P_{COND} = 2\lambda_C \Pi_C \omega_C (T_W - T_{VP}) \frac{\mathrm{sh}(\omega_C L)}{\mathrm{ch}(\omega_C L)} \tag{4}$$

where: λ_C is frame coefficient of conductivity, W/m·K; Π_C – a frame section perimeter, m; T_W – temperature of anemometer wire, K; T_{VP} – vapour flow temperature, K; L – frame length, m;
ω_C parameter is calculated by the expression

$$\omega_C = \sqrt{\frac{\alpha_C \Pi_C}{\lambda_C S_C}} \tag{5}$$

in which α_C is heat transfer coefficient of the frame beams, W/m^2·K; S_C – section area of the frame beams, m^2.

Heat transfer coefficient of the frame beams is calculated in the standard way

$$Nu_C = CPr^n Re_C^i \quad (6)$$

where: $Nu_C = \alpha_C \cdot D_C / \lambda_{VP}$ - Nusselt number of frame beams; $Re_C = \rho_{VP} \cdot u \cdot D_C / \mu_{VP}$ - Reynolds number of frame beams; $Pr = \mu_{VP} \cdot C_P / \lambda_{VP}$ - Prandtl number; D_C - frame beams diameter, m; ρ_{VP} - vapour density, kg/m^3; λ_{VP} - vapor thermal conductivity coefficient, W/m·K; μ_{VP} – vapour coefficient of dynamic viscosity, Pa·s; C_P - vapour heat capacity, J/kg·K; u- vapour flow velocity, m/s; C, n, i – constants depending on beams sectional shape and Reynolds number range Re [3-4]. Conductive participation in heat losses of released capacity P_{COND} reached 18.5 % in this work.

Under stationary conditions the thermal equilibrium of the vapour flow is established for the indicator wire: thermal rating $P_0 - P_{COND}$, heat released when current flows through the wire, is removed by the vapour flow. The type of functional relationship between the wire voltage and the vapour flow average velocity is determined considering the heat exchange process perpendicular to the flow wire and its environment. This process is determined by the empirical relationship:

$$\mathrm{Nu_W} = 0.42\mathrm{Pr}^{0.2} + 0.57\mathrm{Pr}^{0.33}\mathrm{Re_W^{0.5}} \quad (7)$$

where: $Nu_W = \alpha_W \cdot d_W / \lambda_{VP}$ - Nusselt number of the indicator wire; $Re_W = \rho_{VP} \cdot u \cdot d_W / \mu_{VP}$ - Reynolds number of the indicator wire; d_W - small wire diameter, m; α_W - heat transfer coefficient of the wire, W/m^2·K.

For diatomic gases and vapours the expression (7) is true within the Reynolds number range

$$10^{-2} \leq \mathrm{Re} < 10^4 \quad (8)$$

The equation for thermal equilibrium of the anemometer wire is the following:

$$(P_0 - P_{COND}) = \pi L \lambda_{VP} (T_W - T_{VP})\left(0.42\mathrm{Pr}^{0.2} + 0.57\mathrm{Pr}^{0.33}\mathrm{Re_W^{0.5}}\right) \quad (9)$$

where: L – the length of the wire, m.

The hot-wire anemometer measured time average longitudinal components of velocity u of free vapour flow with the wire overheating coefficient 1.8. Calibration was performed using the modified King equation [5,6]

$$\mathrm{u} = \mathrm{k_1}(\mathrm{E}^2 - \mathrm{E_0^2})^{1/\mathrm{j}} + \mathrm{k_2}(\mathrm{E} - \mathrm{E_0})^{1/2} \quad (10)$$

where: E and E_0 - output voltages of the hot-wire anemometer when the vapour is flowing or still, respectively; k_1 , k_2 and j - are constants, determined by calibration. The exponent j is close to 0.45, the second constant k_2 takes into account free convection on the wall at very low velocities of the vapour flow.

The signal from the thread of the hot-wire anemometer is amplified by 10 and input to a 12-digit analog-to-digital converter (ADC) and then to computer, where data is stored in arrays and then processed using standard logarithmic methods. The maximum error when calibrating the hot-wire anemometer does not exceed 10 % of the velocity value u. Measurement error of the time average longitudinal component of vapour flow velocity using the hot-wire anemometer reaches 30 % (± 0.3 m/s).

Measurement results of the vapour flow velocity in the nozzle throat against the thermal head value $\delta T = T - T_B$ on the outer evaporator surface of the HP are shown in the Fig.5 [9-14].

It also shows a comparison between test values of vapour flow velocities (u, m/s), at the nozzle throat (black dots), and in the standard cylindrical vapour channel of the HP (white dots), against the evaporator temperature above the boiling point of diethyl ether, at the equal channel sections. For comparison, the calculated approximate values are plotted: solid line designates the nozzle throat, dotted line designates the cylindrical channel.

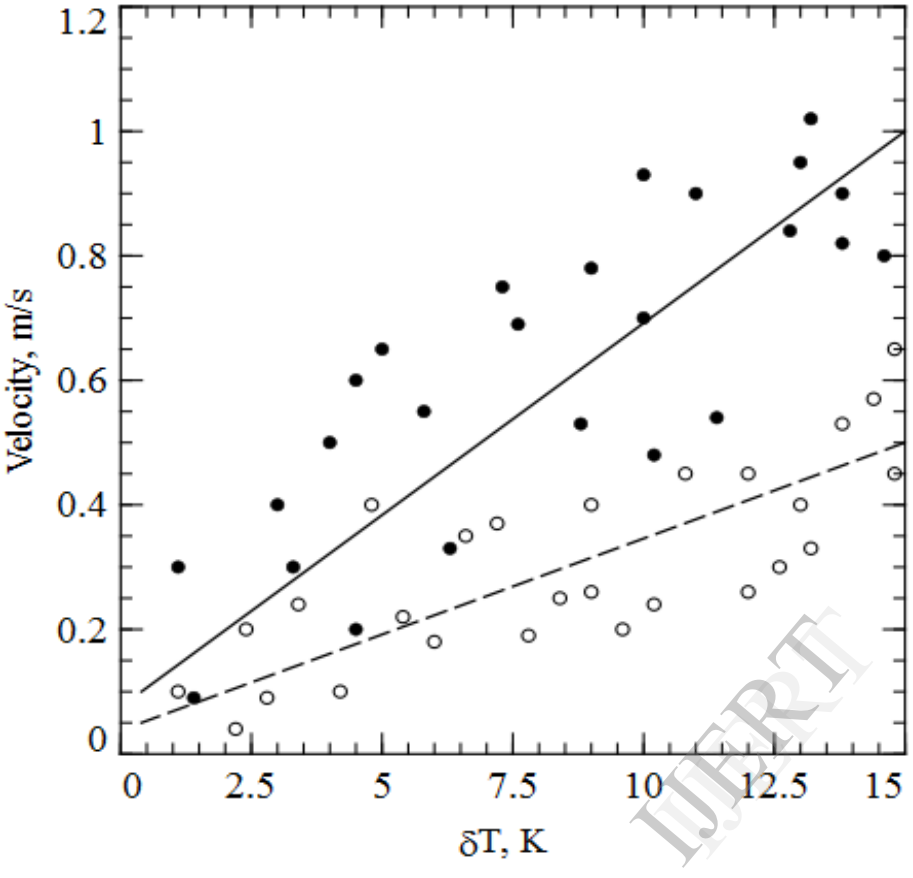

Fig.5. Experimental results of vapour flow velocities.

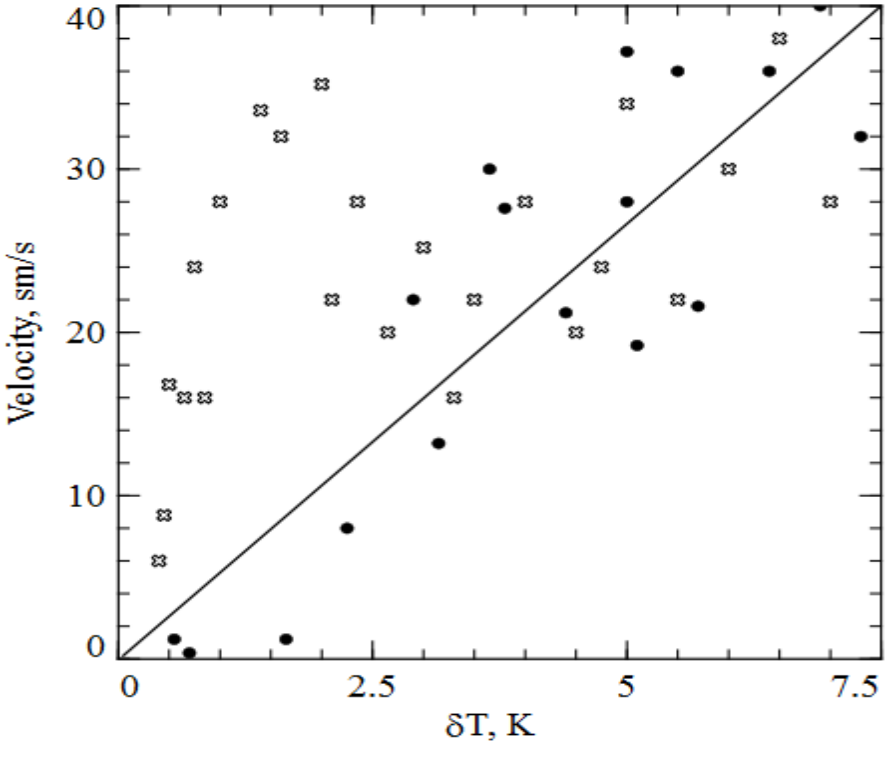

Comparison of tested values of the vapour flow velocities, measured in the nozzle throat, and generated by the evaporator with capillary injector channels (criss-cross), and vapour flow velocities generated by the evaporator without injector channel (solid dots), plotted against the evaporator temperature δT above the boiling temperature of the working fluid (K). Calculated curve of the vapour flow velocity over the evaporator without injector vapour channels is also plotted as a solid line.

Fig. 6. Comparison of the experimental results of vapour flow velocities

Reynolds number Re = 6, Prandtl number Pr = 0.77.

In the preliminary experiments with model equipment it is determined that the condensation intensity of the broadening vapour jet on the perpendicular surface of heat exchange is proportional to the vapour flow vorticity. The motion type of the condensate microdrops in the two-phase dispersed flow is complicated: drops can be accelerated, obtaining additional energy due to not only coagulation but also dispersion of drops into still smaller ones [4,5]. The increase in the condensation nucleus sites of the supersaturated vapour promotes the vapour condensation increase both on the heat exchange surface and on the drops.

Fig.7 and 8 illustrate a strong vapour vortex in the condensation zone of the HP with taper turbulator .

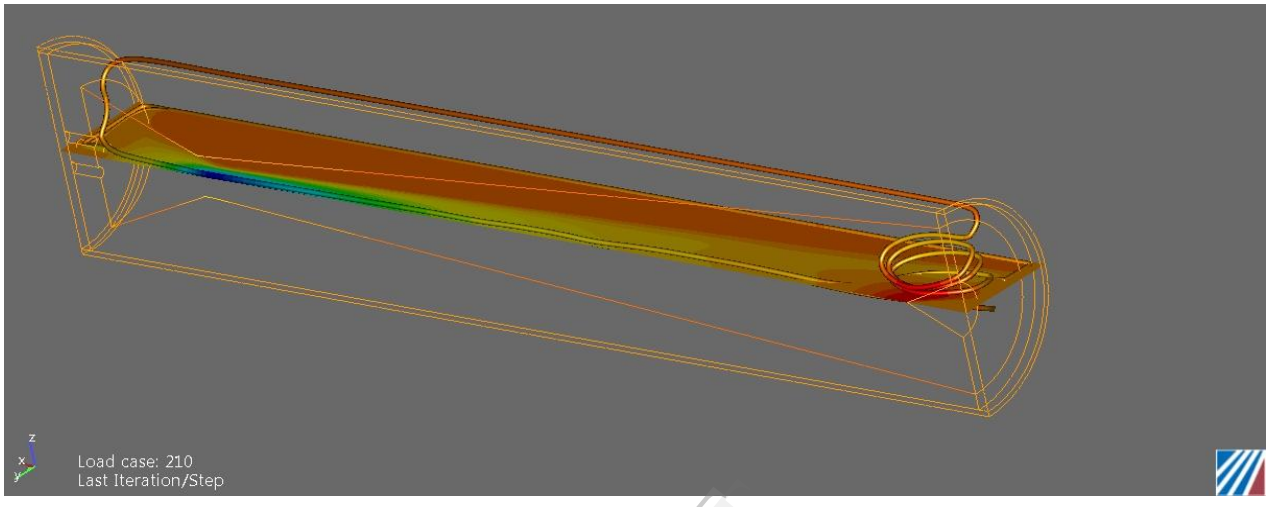

Fig. 7. Vapour jet motion (single jet).

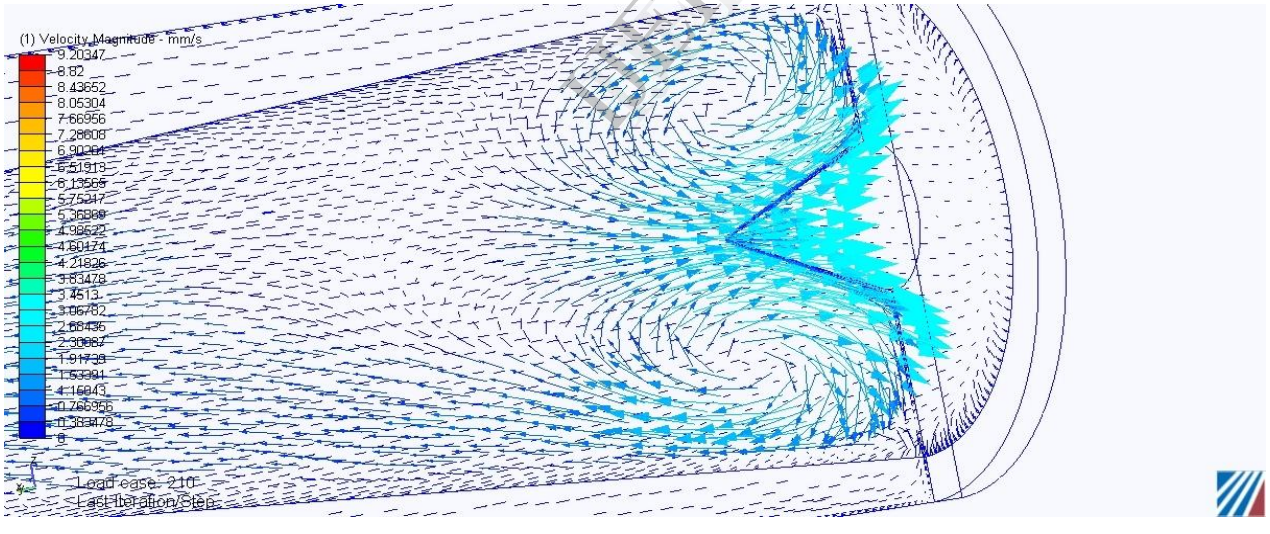

Fig.8. Calculation results of flow velocity of diethyl ether vapour nearby the zone of condensation of HP.

The numerical analysis of the flow in the heat pipe condensation zone shows that the vortex structure has a spatial nature, at the same time the flow asymmetry becomes apparent being determined by non-linear friction against the underlying surface and turbulator and also the two-dimensional vortex compressibility.

Near the underlying surface of the HP condensation zone at the low Reynolds numbers a strongly pronounced boundary layer appears, in which a potential flow component is generated resulting in the circulation in tangential and radial directions.

The vortex structure in the heat pipe condensation zone is affected by non-linear friction against the underlying surface and the boundary layer. These determine both two-dimensional compressibility and flow asymmetry.

The boundary layer is found to be unstable. At present we could not perform the velocity measurements by means of hot-wire anemometer near the turbulator frontal point.

Advantageous features of the Laval nozzle show themselves in the HP, where the motion of the working fluid in the vapour phase is close to convectional, and the problem of intensification of heat transfer characteristics, by means of the flow velocity increase in the vapour channel, is quite important.

It is experimentally confirmed that the flow velocity inside the HP vapour channel, similar to the Laval nozzle, is increased compared to flow velocity inside standard cylindrical vapour channels. This feature is important in the process of industrial manufacturing of short heat pipes.

References

1. Kutateladze S.S. Heat transfer and hydrodynamic resistance/ Handbook. Moscow , «Energoatomizdat». 1990. 367 p.

2. Kutateladze S.S. Principles of heat exchange theory. Edition 5, re-cast and supplemented. Moscow , “Atomizdat». 1979. 416 p.

3. Wang X. Basic forrmulae and heat exchange for engineers: Handbook/ Translation from English. Moscow , «Atomizdat». 1979. 216 p.

4. Zukauskas A.A. Convective heat-transfer in heat exchangers. Moscow, «Nauka», 1982. 472p.

5. Bradshow P. An introduction to turbulence and its measurement. Moscow , 1974. 278 p.

6. Perry A.E. Hot-Wire Anemometry. Oxford: «Clarendon Press». 1982.

7. Glaser A. Observation of traces of fast charged particles in chamber for fluids//UZPECHI FIZICHESKIX NAUK. Moscow. 1954. Vol.52. N.1. p.167-170.

8. GOST 8.563.1-9. Moscow. Russia. Membranes ISA 1932 and Ventury pipes mounted in filled pipelines with round sections. 56 p.

9. Seryakov A.V., Karachinov V.A., Ilyin S.V., Ivshin K.I. Special cooling system of matrix photoreceiving devices.// Proceedings of the 19th International scientific technical conference “Modern television and radioelectronics”. Moscow, FGUP MKB “Electron”. Moscow, 2011. p. 78-79.

10. Seryakov A.V., Konkin A.V., Belousov V.K. The intensification of heat-transfer characteristic of heat pipes.//Proceedings of the VIII Minsk International Seminar of Heat Pipes, Heat Pumps, Refrigerators, Power Sources. Minsk, Belarus, 12-15 September 2011. v 2. p. 59-65.

11. Patent for useful model N.95812 RF, F28D 15/00/Device for heat pipe filling with non - wettable fluid. Seryakov A.V. Published 10.07.2010. Bulletin 19.

12. Patent N 2431101 RF, F 28D 15/00/ Method of heat pipe filling. Seryakov A.V. Published 10.10.2011.Bulletin 28.

13. Seryakov A.V., Konkin A.V., Belousov V.K. Jet velocity increasing in the steam channel of heat pipes of mean temperature range // Reshetnyov reading. Materials of the XVth International scientific conference devoted to the memory of general designer of rocket space systems academician M.F.Reshetnyov. Krasnoyarsk, 2011. Part 1. p.354 - 355.

14. Description of hot-wire thermoanemometer equipment of the DISA company. DISA Type 55A01.2010.